Human water consumption intensifies hydrological drought worldwide

2013 Environ. Res. Lett. 8 034036

(http://iopscience.iop.org/1748-9326/8/3/034036)

OPEN ACCESS
IOP PUBLISHING ENVIRONMENTAL RESEARCH LETTERS
Environ. Res. Lett. **8** (2013) 034036 (14pp) doi:10.1088/1748-9326/8/3/034036

Human water consumption intensifies hydrological drought worldwide

Yoshihide Wada[1], **Ludovicus P H van Beek**[1], **Niko Wanders**[1] and **Marc F P Bierkens**[1,2]

[1] Department of Physical Geography, Utrecht University, Heidelberglaan 2, 3584 CS Utrecht, The Netherlands
[2] Unit Soil and Groundwater Systems, Deltares, Princetonlaan 6, 3584 CB Utrecht, The Netherlands

E-mail: y.wada@uu.nl

Received 24 April 2013
Accepted for publication 17 September 2013
Published 30 September 2013
Online at stacks.iop.org/ERL/8/034036

Abstract
Over the past 50 years, human water use has more than doubled and affected streamflow over various regions of the world. However, it remains unclear to what degree human water consumption intensifies hydrological drought (the occurrence of anomalously low streamflow). Here, we quantify over the period 1960–2010 the impact of human water consumption on the intensity and frequency of hydrological drought worldwide. The results show that human water consumption substantially reduced local and downstream streamflow over Europe, North America and Asia, and subsequently intensified the magnitude of hydrological droughts by 10–500%, occurring during nation- and continent-wide drought events. Also, human water consumption alone increased global drought frequency by 27 (±6)%. The intensification of drought frequency is most severe over Asia (35 ± 7%), but also substantial over North America (25 ± 6%) and Europe (20 ± 5%). Importantly, the severe drought conditions are driven primarily by human water consumption over many parts of these regions. Irrigation is responsible for the intensification of hydrological droughts over the western and central US, southern Europe and Asia, whereas the impact of industrial and households' consumption on the intensification is considerably larger over the eastern US and western and central Europe. Our findings reveal that human water consumption is one of the more important mechanisms intensifying hydrological drought, and is likely to remain as a major factor affecting drought intensity and frequency in the coming decades.

Keywords: human water consumption, hydrological drought, drought intensity, drought frequency, intensification

S Online supplementary data available from stacks.iop.org/ERL/8/034036/mmedia

1. Introduction

Drought is a natural phenomenon caused by below-normal precipitation over a prolonged period (Tallaksen and van Lanen 2004, Wilhite 2000, Mishra and Singh 2010). Lack of precipitation causes a meteorological drought, but results in a hydrological drought as it propagates into more extensive areas along the drainage network (Wilhite and Glantz 1985, Tallaksen and van Lanen 2004). Below-normal water availability in rivers, lakes and reservoirs can cause water scarcity in combination with water demand, threatening water supply and associated food production (Falkenmark *et al* 1997, Döll *et al* 2009, Wisser *et al* 2010).

Various studies analyzed the severity, frequency and trends of hydrological droughts from observed streamflow data (Soulé and Yin 1995, Tallaksen *et al* 1997, Hisdal and Tallaksen 2003, Fleig *et al* 2006, 2011) (table 1).

Table 1. Previous data and model based assessments of hydrological drought.

	Method	Additional components	Data/model	Focus	Duration	Temporal resolution	Spatial resolution
Soulé and Yin (1995)	Palmer hydrologic drought severity index (PHDI)	Linear trend analysis	PHDI records from the National Climate Information Disk (National Climatic Data Center 1990) for 344 climatic divisions	Spatial patterns of temporal trends in drought severity	1895–1989	Year	344 climatic divisions (USA)
Tallaksen *et al* (1997)	Fixed threshold level method ($Q_{50,70,90}$)	Three pooling procedures	2 daily discharge series from 2 catchments with contrasting geology	Threshold level approach with pooling procedures to define drought characteristics	1926–1993	Day	2 catchments (Denmark)
Hisdal *et al* (2001)	Fixed threshold level method (Q_{70})	Trend analysis by the Mann–Kendall test (Mitosek 1995)	2–612 daily discharge series from the European water archive (EWA) (Roald *et al* 1993, Rees and Demuth 2000)	Severity and frequency analysis of drought trends	1911–1995	Day	2–612 discharge stations (Europe)
Hisdal and Tallaksen (2003)	Variable threshold level method	Drought severity–area–frequency curves (Krasovskaia and Gottschalk 1995)	15 daily discharge series from the EWA (Roald *et al* 1993, Rees and Demuth 2000) were expanded by the empirical orthogonal functions (EOF) method (Hisdal and Tveito 1993)	Severity and frequency analysis of drought area	1961–1990	Month	14 km by 17 km (Denmark)
Fleig *et al* (2006)	Variable threshold level method (Q_{20}–Q_{90})	Three pooling procedures	16 daily streamflow series (EU project ASTHyDA; www.geo.uio.no/drought)	Frequency analysis of deficit characteristics	4–92 years	Day	16 discharge stations (Globe)
Timilsena *et al* (2007)	PHDI and Palmer Z index	Cumulative deficit relative to long-term mean to define drought characteristics	3 averaged annual discharge series from 1923 to 2004 (US Geological Survey) were expanded to 500 years by using tree-ring data (Hidalgo *et al* 2000)	Ranking drought characteristics, frequency analysis of drought trends	1493–2004	Annual	Upper Colorado River Basin (USA)
Feyen and Dankers (2009)	Seven-day minimum flows at several recurrence intervals n ($7Qn$)	Generalized extreme value (GEV) distribution (Coles 2001, Katz *et al* 2002)	LISFLOOD (van der Knijff *et al* 2010) with RCM HIRHAM (Christensen *et al* 1996) forcing data	Future drought under the IPCC SRES A2	1961–1990 2071–2100	Day	12 km by 12 km (Europe)
Tallaksen *et al* (2009)	Variable threshold level method (Q_{80})	Average drought deficit volume per event	SWAP coupled with MODFLOW (Peters *et al* 2006)	Groundwater recharge, head and discharge	1961–1997	Month	500 m × 500 m (UK)

Table 1. (Continued.)

	Method	Additional components	Data/model	Focus	Duration	Temporal resolution	Spatial resolution
Döll *et al* (2009)	Statistical monthly low flow (Q_{90})	—	WaterGAP (Alcamo *et al* 2003b, 2003a) with CRU TS2.1 (Mitchell and Jones 2005) and GPCC (Fuchs *et al* 2008) forcing data	Low flow associated with six ecologically relevant indicators	1961–1990	Month	0.5° (Globe)
Corzo Perez *et al* (2011)	Fixed threshold level method (Q_{80})	Non-contiguous and contiguous drought area analysis	WaterGAP (Alcamo *et al* 2003b, 2003a) with WATCH forcing data (Weedon *et al* 2011)	Subsurface runoff	1963–2001	Day	0.5° (Globe)
Fleig *et al* (2011)	Variable threshold level method (Q_{70}–Q_{90})	Regional drought area index (RDAI)	58 daily discharge series from national databases	Drought development in relation to antecedent weather types (WTs)	1964–2000	Day	58 discharge stations (UK and Denmark)
van Loon and van Lanen (2012)	Variable threshold level method (Q_{80})	Pooling procedure (Zelenhasić and Salvai 1987)	HBV (Seibert 1997) with observed meteorological forcing data	Distinguish six drought types in relation to climate	1960–2007	Day	5 catchments (Europe)

Although hydrological drought is preferably analyzed using streamflow observations (Corzo Perez *et al* 2011), such observations are generally not available at large spatial extents and for long temporal coverage, though hydrological drought can be as extensive as regional to continental scales. Recent developments in large-scale hydrological modeling enabled the analysis of drought over much larger extents, e.g. continental (Tallaksen *et al* 2009, Feyen and Dankers 2009, van der Knijff *et al* 2010, van Loon and van Lanen 2012, Hisdal *et al* 2001) to global scale (Corzo Perez *et al* 2011, van Huijgevoort *et al* 2012), and over longer timeframes, e.g. past reconstructions and future projections (Andreadis *et al* 2005, Sheffield and Wood 2007). These model studies identified drought characteristics primarily for pristine conditions (natural streamflow) such that anthropogenic influence (human water consumption) on resulting drought is not explicitly considered.

Recent studies by Dai (2011, 2013) and Sheffield *et al* (2012) suggest that anthropogenic global warming is likely responsible for intensifying meteorological droughts, e.g. enhanced evaporative demand and altered monsoon circulation over regions such as Africa and Asia. However, it remains unclear to what degree human water consumption intensifies hydrological droughts worldwide. Over the past decades, human water consumption has more than doubled, primarily due to a large increase in irrigation water demand (Wisser *et al* 2010), and affected streamflow over various regions (Döll *et al* 2009, Wisser *et al* 2010). It can thus be expected that there is a substantial anthropogenic impact on hydrological drought in many parts of the world.

Distinct from water scarcity assessments (Falkenmark *et al* 1997, Wada *et al* 2011b), the intensification of hydrological droughts, i.e. drought intensity and frequency, due to human water consumption can occur even in water-rich regions or areas with no local water consumption as a result of upstream human water consumption. Our study stands out from earlier work in that it presents for the first time the anthropogenic impact on hydrological droughts over the period 1960–2010 that extends beyond most global analyses.

2. Methods, model and data

2.1. Hydrological drought definition and standardized drought deficit volume

The commonly used variable threshold level method was used to identify below-normal water availability as the onset of hydrological droughts (Hisdal and Tallaksen 2003, Fleig *et al* 2006). We selected the monthly 80-percentile flow, Q_{80}, i.e. the mean monthly streamflow that is exceeded 80% of the time, as the threshold level, which accounts for seasonal streamflow variability (Hisdal *et al* 2001, Andreadis *et al* 2005, Sheffield and Wood 2007, Tallaksen *et al* 2009, Corzo Perez *et al* 2011, van Loon and van Lanen 2012). The selected 80-percentile flow lies between 70- and 95-percentile flow commonly used in drought analysis for perennial rivers (Tallaksen *et al* 1997, Hisdal and Tallaksen 2003, Fleig *et al* 2006, 2011, Tallaksen *et al* 2009, van Loon and van Lanen 2012, Hisdal *et al* 2001, van Huijgevoort *et al* 2012). Drought intensity is determined in terms of the deficit volume below the threshold levels (Hisdal *et al* 2001, Tallaksen *et al* 2009, Corzo Perez *et al* 2011, van Loon and van Lanen 2012). Although this method potentially creates missing values for ephemeral streams where $Q_{80} = 0$, this problem is less obvious in our analysis since we used monthly rather than daily streamflow series.

To allow comparison between rivers of different size, we standardized the deficit volume by dividing it by Q_{80} or the threshold level to express the relative intensity of drought conditions to normal streamflow conditions or Q_{80}.

$$\mathrm{Dfv}_{i,m} = \max(0, \tau_{i,m} - Q_{i,m}) \quad (1)$$

$$\mathrm{SDfv}_{m,i} = \frac{\mathrm{Dfv}_{m,i}}{\tau_{m,i}} \quad (2)$$

where Dfv is the deficit volume, τ is the threshold ($Q_{80m,i}$), Q is the simulated streamflow, and SDfv is the standardized deficit volume. Subscripts i and m denote per grid cell (0.5°) and per month respectively.

Drought frequency was derived by counting the occurrences of drought events, i.e. when streamflow falls below the threshold Q_{80}, and it was indexed by dividing it by the average frequency over the period 1960–2010 for pristine conditions to express the relative increase due to human water consumption.

In addition, the population size experiencing below 80% of normal streamflow conditions (Q_{80}) was calculated as a measure of the number of persons affected by severe hydrological droughts per year. This population size was calculated per grid cell, but was summed over the globe and for each continent. The selection of the threshold is rather arbitrary, but is based on the experience that 80% of normal streamflow condition or rainfall amount historically causes severe drought conditions (Wilhite 2000, Wilhite and Glantz 1985).

2.2. Analysis of drought intensification due to human water consumption

To assess the impact of human water consumption on drought intensity and frequency, we performed three analyses (table S1 in the supplement available at stacks.iop.org/ERL/8/034036/mmedia). The first run evaluates streamflow under climate variability and with no human water consumption (hereafter, pristine), while the second run evaluates streamflow under variable climate inputs and with human water consumption set to the level of 1960 (hereafter, 1960 consumption), and the third run is subject to the reconstructed water consumption over 1960–2010 (hereafter, transient consumption). We calculated Q_{80} or the threshold values from simulated mean monthly streamflow (i.e., river discharge) under pristine conditions over the period 1960–2010. The threshold level Q_{80} derived from the pristine condition was then used to compute the deficit volumes for streamflow subject to varying degrees of human water consumption: pristine conditions, 1960 consumption and transient consumption. The increase in ensuing deficit

volumes calculated compared to the pristine condition is thus an indicative of the anthropogenic intensification of hydrological drought. From these runs, we also analyzed the frequency of hydrological droughts as a result of human water consumption relative to the pristine conditions, and calculated the number of people affected by hydrological droughts worldwide over the period 1960–2010.

2.3. Model simulation of streamflow

The state-of-the-art global hydrological and water resources model PCR-GLOBWB was used to simulate spatial and temporal continuous fields of streamflow and storage in rivers, lakes, reservoirs and wetlands at a 0.5° spatial resolution for the period 1960–2010 (Wada *et al* 2010, van Beek *et al* 2011). In brief, the model simulates for each grid cell and for each time step (daily) the water storage in two vertically stacked soil layers and an underlying groundwater layer. At the top a canopy with interception storage and a snow cover may be present. Snow accumulation and melt are temperature driven and modeled according to the snow module of the HBV model (Bergström 1995). To represent rain–snow transition over sub-grid elevation dependent gradients of temperature, ten elevation zones was made on each grid cell based on the HYDRO1k Elevation Derivative Database, and scaled the 0.5° grid temperate fields with a lapse rate of 0.65 °C 100 m^{-1}. The model computes the water exchange between the soil layers, and between the top layer and the atmosphere (rainfall, evaporation and snowmelt). The third layer represents the deeper part of the soil that is exempt from any direct influence of vegetation, and constitutes a groundwater reservoir fed by active recharge. The groundwater store is explicitly parameterized and represented with a linear reservoir model (Kraaijenhoff van de Leur 1958). Sub-grid variability is taken into account by considering separately tall and short vegetation, open water (lakes, reservoirs, floodplains and wetlands), soil type distribution (FAO Digital Soil Map of the World), and the area fraction of saturated soil calculated by the Improved ARNO scheme (Hagemann and Gates 2003) as well as the spatio-temporal distribution of groundwater depth based on the groundwater storage and the surface elevations as represented by the 1 km × 1 km Hydro1k data set.

The model runs with a daily time step, but simulated streamflow is evaluated per month for this study. Simulated specific runoff from the two soil layers (direct runoff and interflow) and the underlying groundwater layer (base flow) is routed along the drainage network based on DDM30 (Döll and Lehner 2002) by using the kinematic wave approximation of the Saint-Venant equation (Chow *et al* 1988). The effect of open water evaporation, storage changes by lakes, and attenuation by floodplains and wetlands are taken into account. Streamflow may be reduced by upstream human water consumption from all sectors (households, industry and agriculture). When in a grid cell the available streamflow is less than the water consumption, no streamflow returns. Otherwise, the streamflow in excess of the local water consumption is accumulated along the drainage network.

A reservoir operation scheme is also implemented, which is dynamically linked with the kinematic routing module. This reservoir scheme optimizes for each reservoir the release given its purpose by defining the monthly target storage for the next two operational years to ensure its proper functioning given the forecasts of inflow and downstream demand along the drainage network. The target storage determines the daily outflow from reservoirs, and is updated as actual daily inflow and demand start to deviate from the long-term expected value. Four types of reservoir operations are distinguished on the basis of the reservoir data from the GLWD dataset (Lehner and Döll 2004), being water supply, flood control, hydropower generation, and others (e.g., navigation). In total we considered 513 reservoirs of the 654 reservoirs included in the GLWD dataset for the world's largest reservoirs (storage capacity $\geq$ 0.5 km^3). The selected reservoirs represent 94% of the area of 255 109 km^2 and 95% of the capacity of 4615 km^3 contained by the GLWD dataset. The missing reservoirs cannot be truthfully represented given their limited size and catchment area and the required information on their purpose and characteristics is lacking.

The model was forced with daily fields of precipitation, reference (potential) evapotranspiration and temperature. For the period 1960–2000, precipitation and temperature were prescribed by the CRU TS 2.1 monthly data set (Mitchell and Jones 2005), which was subsequently downscaled to daily fields by using the ERA40 re-analysis data (Uppala *et al* 2005). The precipitation data was corrected for snow undercatch bias over the Northern Hemisphere (Adam and Lettenmaier 2003). Over the same time period, prescribed reference evapotranspiration was calculated based on the Penman–Monteith equation according to the FAO guidelines (Allen *et al* 1998) using the time series data of CRU TS 2.1 with additional inputs of radiation and wind speed from the CRU CLIM 1.0 climatology data set (New *et al* 2002). This was subsequently downscaled to daily fields on the basis of the daily temperature from the ERA40 re-analysis data. To extend our analysis to the year 2010, we forced the model by a comparable daily climate fields taken from the ERA-Interim re-analysis data (Dee *et al* 2011). We obtained daily fields of GPCP-corrected precipitation and temperature (GPCP: Global Precipitation Climatology Project; www.gewex.org/gpcp.html), and calculated reference evapotranspiration by the same method retrieving relevant climate fields from the ERA-Interim dataset. For compatibility with our overall analysis, we bias-corrected this dataset (precipitation, reference evapotranspiration and temperature) by scaling the long-term monthly means of these fields to those of the CRU TS 2.1 data set, wherever station coverage by the CRU is adequate ($\geq$2 stations). Otherwise the original ERA-Interim data were returned by default.

2.4. Calculating human water consumption

Over the period 1960–2010, human water consumption, i.e. water withdrawal minus return flow, was reconstructed at monthly time steps on a 0.5° global grid for agricultural

(livestock and irrigation), industrial and domestic sectors using the latest available data on socio-economic (e.g., total, urban and rural population, Gross Domestic Product and access to water), technological (e.g., energy and household consumption and electricity production) and agricultural (e.g., the number of livestock, irrigated areas, crop factor and crop growing season) drivers (Wada *et al* 2011a, 2011b). Return flow from water that is withdrawn was assumed to occur to the river system on the same day. Neither water retention due to waste water treatment nor the degradation of water quality after water is withdrawn was considered in this study. However, the quality of water is generally degraded after water is withdrawn particularly in regions with limited sewage and water treatment facilities. This effect is partly accounted for by including the number of population who have access to water, which was used to calculate the amount of return flow from the domestic sector (Wada *et al* 2011a). Nevertheless, water pollution affects the amount of readily available water over a region and the calculation presented here may potentially underestimate the human impact (i.e., water quality) on hydrological drought.

When estimating sectoral water consumption we explicitly accounted for nonrenewable groundwater abstraction (groundwater abstraction minus groundwater recharge) and desalinized water use as an additional source of human water consumption that is not imposed on the renewable water resources (streamflow). Note that nonrenewable groundwater abstraction is estimated with a simplistic, flux based, approach (Wada *et al* 2012) and the model does not consider increased capture due to decreased groundwater discharge and increased recharge from surface waters due to groundwater pumping (Bredehoeft 2002, Shamsudduha *et al* 2011). The actual amount taken from the simulated streamflow is then the minimum of the estimated net total consumptive water use, i.e. total consumptive water use minus nonrenewable groundwater abstraction and desalinated water use, and the available streamflow, already diminished with any upstream consumption. The calculated human water consumption has been validated in earlier work (Wada *et al* 2011a).

A map of estimated total human water consumption from domestic, industrial, agricultural sectors for the year 2010 is shown in figure S1 (see supplementary material available at stacks.iop.org/ERL/8/034036/mmedia). Estimated global water consumption totals 1970 $km^3\ yr^{-1}$, where the agricultural sector consumes the largest amount, 1403 $km^3\ yr^{-1}$, with industrial and domestic sector consuming 294 and 273 $km^3\ yr^{-1}$, respectively. Over the period 1960–2010, human water consumption increased almost two and a half times. This increase is attributable to a drastic rise in irrigation water consumption, which almost doubled over the past 50 years (from 828 to 1403 $km^3\ yr^{-1}$). However, industrial water consumption nearly tripled over that period (from 116 to 294 $km^3\ yr^{-1}$), while domestic (households') water consumption more than quintupled (from 57 to 273 $km^3\ yr^{-1}$) due to rapid population growth and increased standard of living.

3. Results

3.1. Comparison of simulated and observed drought deficit volumes

Figure 1 compares simulated drought deficit volumes as calculated under pristine conditions and under transient human water consumption, with those calculated from observed streamflow. We selected 23 large river basins over different climate zones of the world, and considered drought events for each available GRDC station along these rivers. Figure 1(a) provides a scatter plot of all events of all rivers. Under pristine conditions, the simulated deficit volumes are underestimated with α (slope or regression coefficient) of 1.3 and R^2 (the coefficient of determination) $= 0.5$ (p-value < 0.001). Under transient human water consumption, α becomes close to 1 with $R^2 = 0.75$ (p-value < 0.001). Including human water consumption results in smaller deviations between simulated and observed deficit volumes per drought event, and significantly reduced the residual variance of simulated deficit volumes (pristine over transient) (F-test $= 1.2$, p-value < 0.05). We also tested whether the change in those slopes ($1.3 \rightarrow \sim 1.0$) indicates statistically a significant improvement in terms of simulated deficit volumes based on an analysis of variance (ANOVA). The residual variances of both simulations (pristine conditions and transient consumption) are adjusted in advance, assuming equal residual variances. The results rejected both line coincidence (F-test > 100, p-value < 0.001) and line parallelism (t-test < -7, p-value < 0.001), but show nearly equal intercepts (t-test ≈ 0.92, p-value > 0.25). These results indicate that the improvement in simulated deficit volumes after accounting for human water consumption is statistically significant. We then considered for extreme drought events whether this improvement is also evident. Extreme events were particularly chosen because they are usually related to meteorological extreme and the human impact on such drought events is less well known. We compared simulated and observed deficit volumes for the five worst drought events per river basin (figure 1(b)). The (cumulative) frequency distributions of R^2 and α show that under transient human water consumption more than half of the rivers have R^2 over 0.6 and α between 0.75 and 1.25 respectively, while under pristine conditions, half of the rivers have R^2 just above 0.2 and α between 0.5 and 1.5 respectively. These results clearly show the importance of human water consumption in explaining observed both minor and major hydrological drought events. Further validation and discussion including basin-specific statistics are given in table S2 and figure S2 (see supplementary material available at stacks.iop.org/ERL/8/034036/mmedia).

3.2. Human intensification of hydrological drought intensity

We compared, for several exceptional nation- and continent-wide drought events, simulated standardized deficit volumes under pristine conditions with those subject to transient human water consumption (figure 2 and S3 available at stacks.iop.org/ERL/8/034036/mmedia). Over North America,

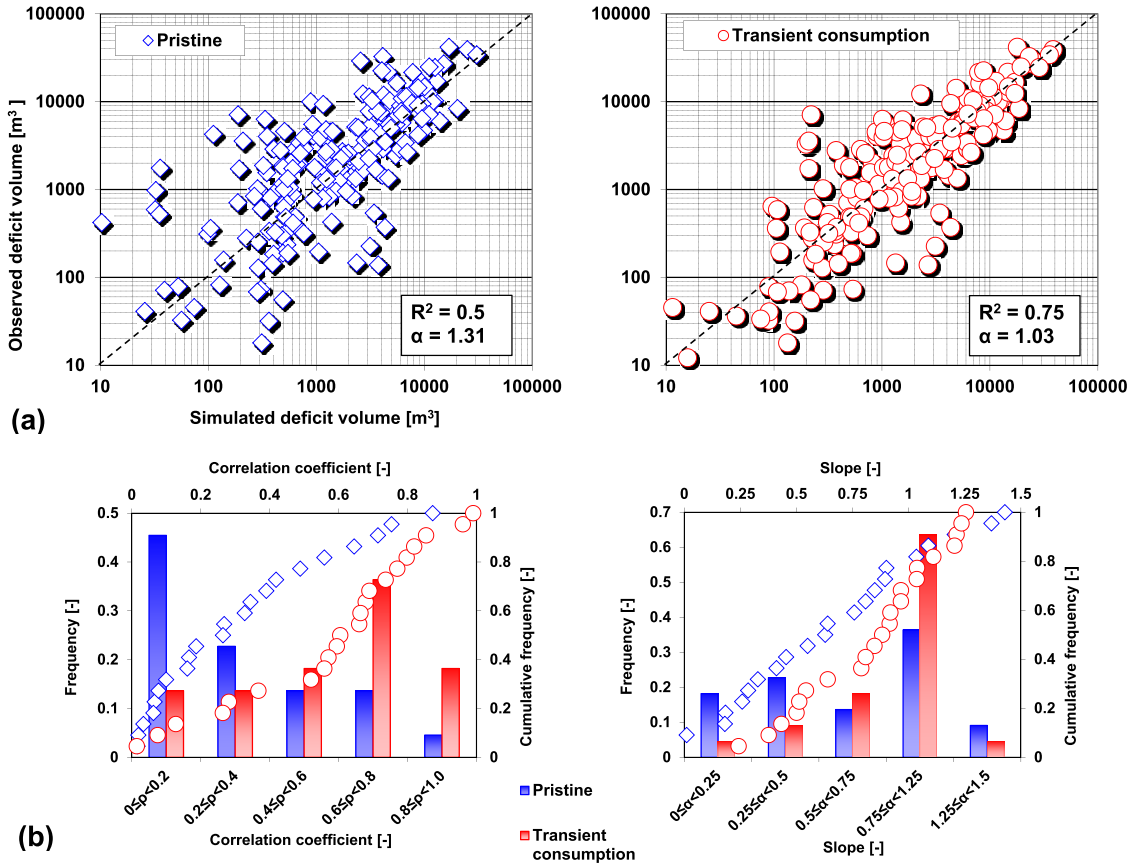

Figure 1. (a) Comparison of per drought event simulated deficit volumes (m^3) under pristine conditions (climate variability only) and under transient human water consumption with those calculated from observed streamflow in a logarithmic scale over 23 major river basins that are affected by human water consumption. The observed streamflow was taken from the selected GRDC stations closest to outlets. (b) Frequency distribution of correlation coefficient and slope per river basin from (a). Five worst drought events were selected from each of 23 major river basins. Note that for fair comparison, deficit volume was calculated with the threshold level Q_{80} that was derived respectively from each streamflow time series: from the GRDC observations; from the simulated streamflow under pristine conditions; from the simulated streamflow under transient human water consumption. River basins (GRDC stations; station number; available period used) selected: Orinoco (Puente Angostura; 3206720; 1960–1990), Parana (Corrientes; 3265300; 1960–1992), Nile (El Ekhsase; 1362100; 1973–1985), Blue Nile (Khartoum; 1663100; 1960–1983), White Nile (Malakal; 1673600; 1960–1996), Orange (Vioolsdrif; 1159100; 1964–1987), Zambezi (Katima Mulilo; 1291100; 1964–2002), Murray (below Wakool Junction; 5304140; 1960–2002), Mekong (Mukdahan; 2969100; 1960–1994), Brahmaputra (Bahadurabad; 2651100; 1969–1993), Ganges (Hardinge Bridge; 2646200; 1965–1993), Indus (Kotri; 2335950; 1967–1980), Yangtze (Datong; 2181900; 1960–1989), Huang He (Sanmenxia; 2180700; 1960–1989), Mississippi (Vicksburg; 4127800; 1960–2000), Columbia (The Dalles; 4115200; 1960–2000), Mackenzie (Norman Wells; 4208150; 1961–2002), Colorado (Yuma; 4152050; 1965–1990), Volga (Volgograd Power Plant; 6977100; 1960–2002), Dnieper (Dnieper Power Plant; 6980800; 1960–1985), Danube (Ceatal Izmail; 6742900; 1960–2002), Rhine (Rees; 6335020; 1960–2002), Elbe (Wittenberge; 6340150; 1960–2002).

particularly the US, the 1988 (figure S3) and 2002 (figure 2) droughts were among the worst, primarily due to a persistent El Niño–Southern Oscillation (ENSO), with record low rainfalls during spring and summer (Trenberth *et al* 1988, Seager 2007). Our results show that with human water consumption drought intensities increased substantially by 50%–500% over the western, central, and eastern US, southern Canada, and central Mexico, where human water consumption appears to be the main driver causing the drought event for both years. Over Europe, the intensification of drought conditions is milder than that over the US due to lower human water consumption, but it is still substantial over central and southern parts of the region under major drought events such as those of 1976, and 2003. Over these regions, the drought conditions are driven primarily by human water consumption. We find that the intensification of droughts is driven by industrial and households' water consumption (≈70–90% of total water consumption) over west-central Europe, including the UK, Germany, France and The Netherlands, while it is caused primarily by irrigation water consumption (>70% of total consumption) over southern Europe, including Spain, Italy, and Greece. The magnitude of the intensification is 10%–200% for the year 1976, but it rises to 40%–300% due to increased human water consumption for the year 2003. Over Asia, during the major drought of 2001, the intensification of droughts was most severe over India, Pakistan, Afghanistan, Uzbekistan, Turkmenistan, and north-eastern China, where irrigation water consumption exceeds 90% of total water used (Wada *et al* 2012). For these regions, drought intensities increased by 200%–500% as a result of substantially reduced local and downstream flow. Importantly, severe drought conditions over India and

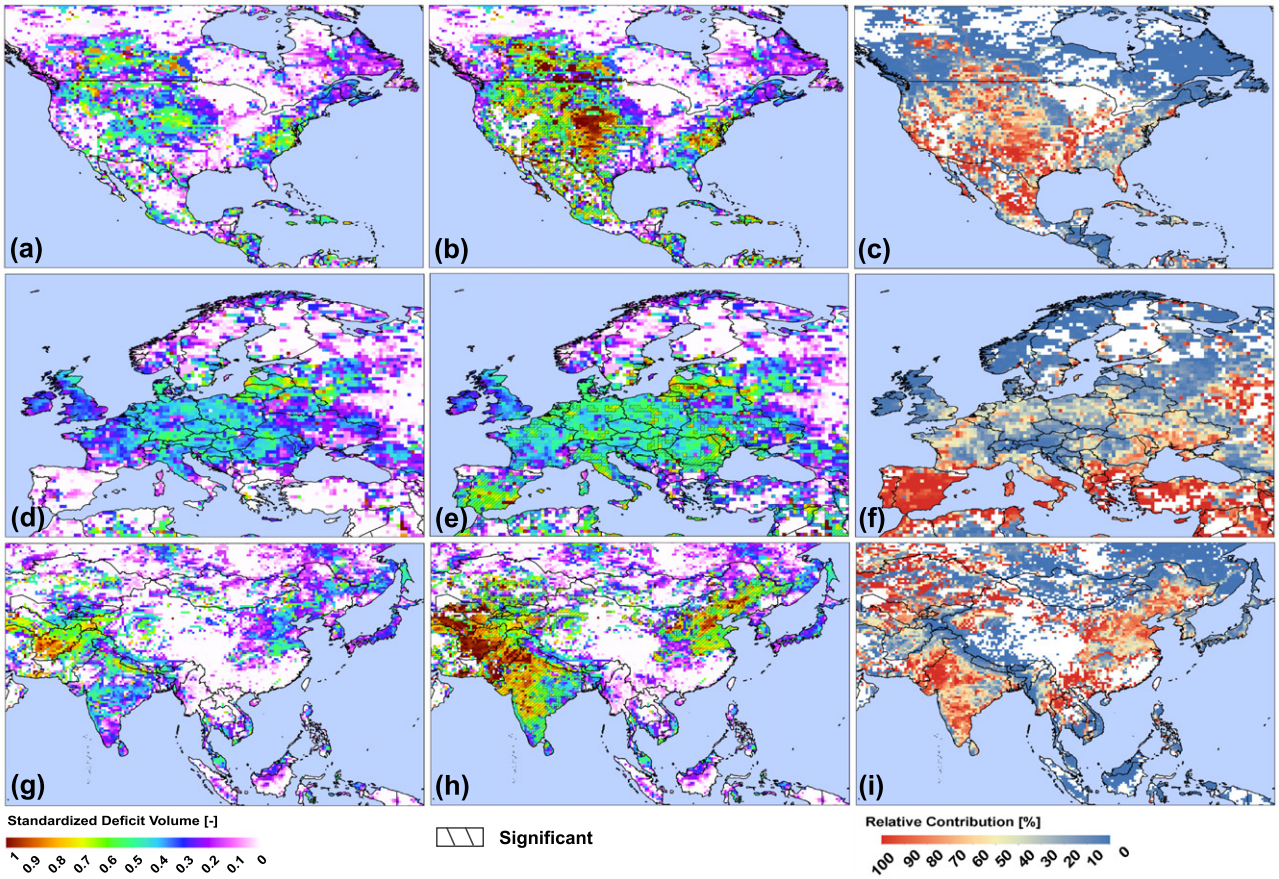

Figure 2. Comparison of standardized deficit volumes (—) with (left) pristine condition and with (middle) transient human water consumption, and (right) relative contribution of human water consumption (%) for major drought events over (a)–(c) North America (2002), (d)–(f) Europe (2003), and (g)–(i) Asia (2001). We tested whether the change due to human water consumption is significant by calculating the standard error from observed and simulated standardized deficit volume (under transient human water consumption) for all drought events over each basin (see supplementary material, available at stacks.iop.org/ERL/8/034036/mmedia). We used the average standard error over all basins as an estimate for all drought events. We then compared the change to two times average standard error (p-value < 0.05) to test the significance. Areas with significant change are highlighted with dark-gray lines.

Pakistan are driven by human water consumption, whereas those over Afghanistan and Turkmenistan are caused by climatic conditions. For selected droughts in Oceania (2006), human water consumption has smaller impacts over limited areas, with the strongest impact over the Murray-Darling basin, where droughts intensified by 20%–200% due to large irrigation water consumption (figure S3). Over South America (2010) and Africa (1984) the impact of human water consumption during drought events is limited, except for several countries where human water consumption is still substantial, such as Egypt, South Africa, Chile, and Argentina (>10 km^3 yr^{-1}).

3.3. Human intensification of hydrological drought frequency

Figure 3 compares the evolution of drought frequency under pristine conditions (climate variability only), with that under 1960 water consumption, and under transient water consumption, over the globe and for each continent. Trends of drought frequency under pristine conditions reflect multi-decadal climate variability, with globally a decrease of frequency from the 1960s into the 1980s and an increase thereafter. This global signal is from a combination of drought frequency in North America (high frequency–low frequency–high frequency), South America (high–low), Oceania (high–low–high) and Africa (increasing frequency) over the period 1960–2010 (Sheffield and Wood 2011). The result shows that already around 1960 drought frequency was considerably enhanced by human water consumption. The widening gap in drought frequency between 1960 water consumption and transient water consumption indicates the intensification of drought frequency as a result of increased human water consumption over the period 1960–2010. In 2010, the global drought frequency of transient water consumption is higher by 27 (±6)% compared to pristine conditions. Human water consumption increases drought frequency by 35 (±7)% for Asia, by 20–25 (±5–6)% for North America and Europe and by 10–20 (±2–3)% for South America, Africa, and Oceania. Included in figure 3 is the population size (per year) experiencing conditions under 80% of normal streamflow for any given month during that

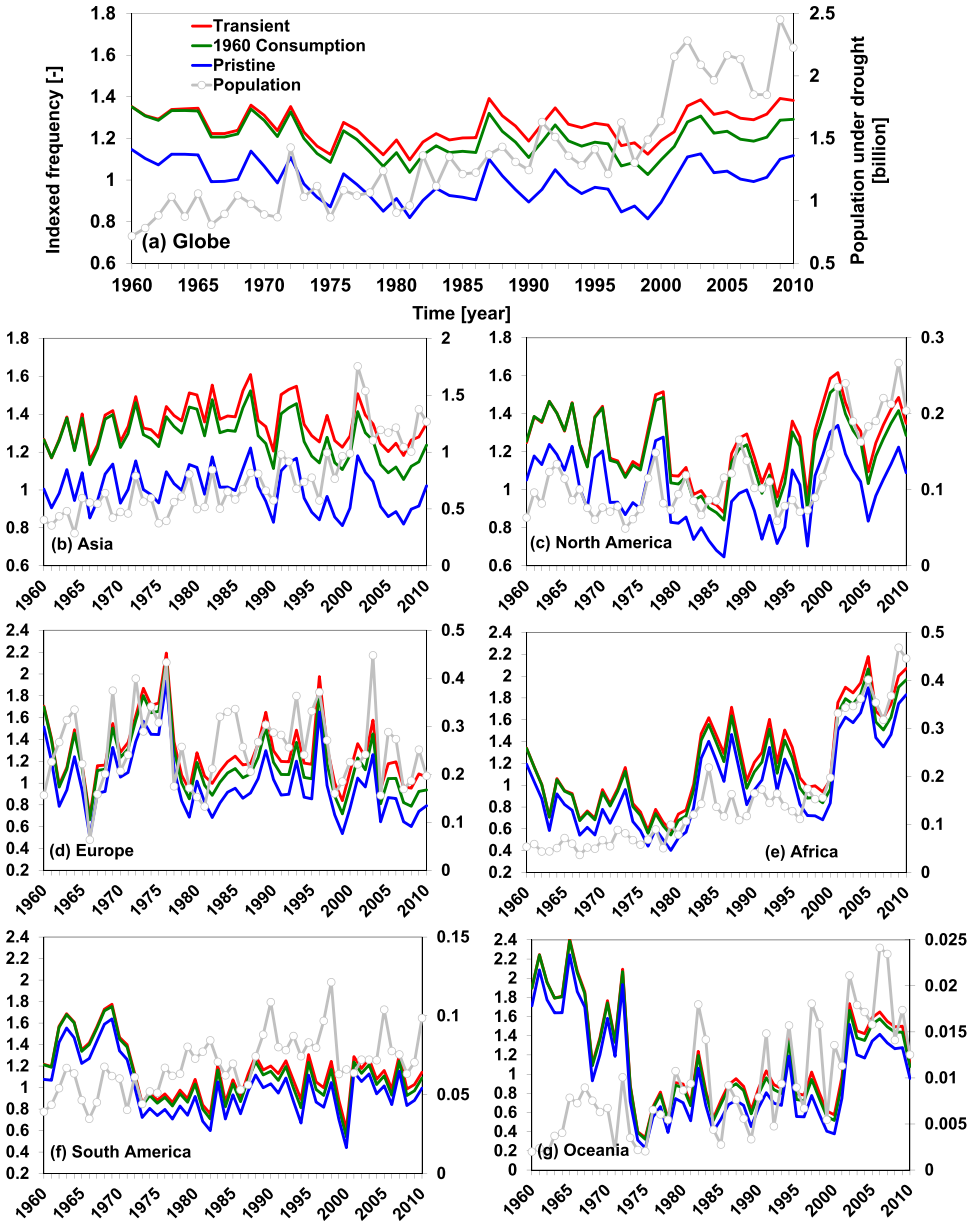

Figure 3. Time series of estimated global hydrological drought frequency with pristine conditions (climate variability only), with fixed consumptive water use of 1960 (1960 consumption), and with transient consumptive water use (transient consumption) over the period 1960–2010 over (a) the Globe, and for each continent; (b) Asia, (c) North America, (d) Europe, (e) Africa, (f) South America, and (g) Oceania. The frequency was derived from the sum of the number of drought events below threshold levels for each year over the globe and for each continent. The frequency was indexed per year by dividing the sum by the average drought frequency of the pristine condition over the period 1960–2010. Population under 80% of normal streamflow condition is plotted per year. Annual country population data was taken from FAOSTAT (http://faostat.fao.org/), and was spatially downscaled to 0.5° spatial resolution (Wada *et al* 2011b).

particular year. Results are shown for the run with transient consumption. Although the increase in drought frequency is mild over the period 1960–2010, the global population under drought substantially increased from 0.7 billion in 1960 to 2.2 billion in 2010. This increase is primarily driven by rapid population growth and increased population density (per grid cell). At a regional scale, similar trends are found for Asia, North America, Africa, South America, and Oceania, where population numbers are steadily increasing. These results suggest that more and more people are vulnerable to droughts, despite the relatively regular drought occurrence over time. In Africa, the population under drought increased dramatically by 10 times from 50 million in 1960 to 500 million in 2010 due to both increased drought occurrence and population growth.

To investigate the sensitivity of estimated drought frequency (figure 3) to the different percentile threshold levels (Q_{70}, Q_{80}, and Q_{90}), in figure 4 we plotted the evolution of drought frequency under pristine conditions and under transient water consumption that was derived with each percentile threshold over the period 1960–2010. The results indicate that indexed drought frequency under pristine

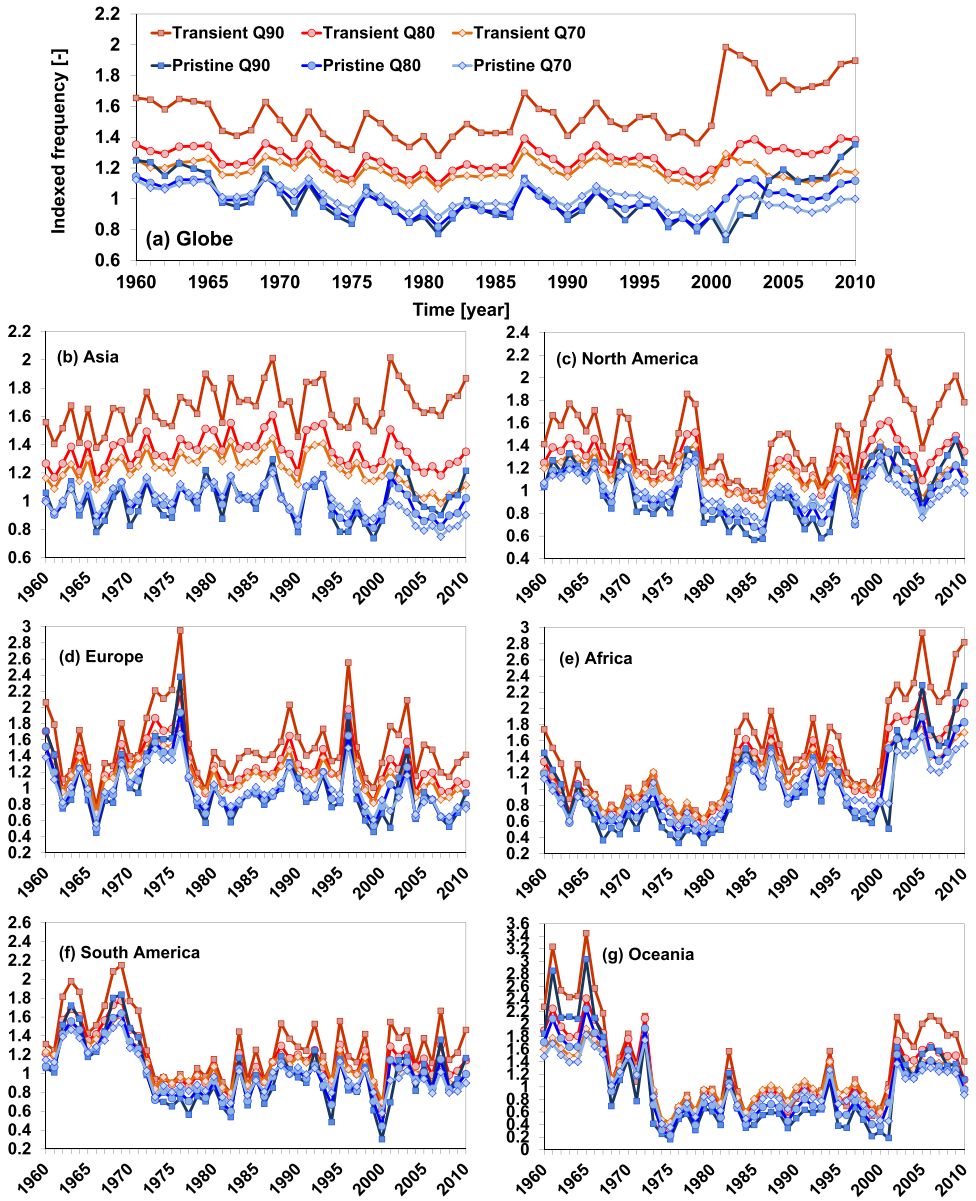

Figure 4. Sensitivity of estimated hydrological drought frequency (figure 3) to the different percentile thresholds (Q_{70}, Q_{80}, and Q_{90}) for pristine conditions (climate variability only) and for transient consumptive water use (transient consumption) over the period 1960–2010 over (a) the Globe, and for each continent; (b) Asia, (c) North America, (d) Europe, (e) Africa, (f) South America, and (g) Oceania. The frequency was derived from the sum of the number of drought events below threshold levels (Q_{70}, Q_{80}, and Q_{90}) for each year over the globe and for each continent. The frequency was indexed per year by dividing the sum by the average drought frequency of the pristine condition calculated with each percentile threshold over the period 1960–2010.

conditions appear to be insensitive to the choice of the percentile threshold levels, although the absolute number of drought occurrence generally increases with higher percentile thresholds ($Q_{90} \rightarrow Q_{70}$). However, for transient consumption, indexed drought frequency tends to be higher with the lower percentile thresholds ($Q_{70} \rightarrow Q_{90}$) and the absolute number of drought occurrence also increase with higher percentile thresholds ($Q_{90} \rightarrow Q_{70}$). This trend is especially obvious for drought frequency calculated with Q_{90}, that substantially deviates from those calculated with Q_{80} and Q_{70}. These results suggest that the calculation of drought frequency appears to be sensitive to the choice of percentile threshold level ($<Q_{80}$) and the inclusion of human water consumption.

4. Discussion

This study reveals that the magnitude of hydrological drought intensity and frequency is largely underestimated when using streamflow under pristine conditions that have been widely used for model based hydrological drought assessments. When comparing nation- and continent-wide drought events simulated under pristine conditions and transient human water consumption, human water consumption intensifies the drought intensity by 10%–500%. The intensification is mainly attributable to irrigation which requires a large amount of water during cropping period, and reduces substantially downstream streamflow. However, the impact of

industrial and households' water consumption on the drought intensification is substantial over the eastern US and western and central Europe.

Such intensified droughts likely have detrimental effects on our society and ecosystems, causing persistent low flow conditions. To briefly address the societal and environmental impacts of intensified hydrological droughts, we conducted a first-order analysis on cooling in thermal power plants (∼stream discharge), navigation (∼stream water height), and aquatic ecosystems (∼stream temperature) (see supplementary material for further details, available at stacks.iop.org/ERL/8/034036/mmedia). Figure S4 (available at stacks.iop.org/ERL/8/034036/mmedia) depicts the results of intensified hydrological droughts: (1) stream temperature increase due to decreased streamflow, (2) potential decrease in the amount of water available for cooling thermal power plants, and (3) decrease in stream water height due to reduction in streamflow. Water supply in populated regions with large households' water consumption, such as western and eastern US, central Mexico, and many parts of Asia, is also likely impacted (MacDonald 2010, Gleick 2010, Pederson 2012).

Part of the decreased streamflow can be buffered by increasing reservoir release in regions where infrastructure (e.g., dams) is present. The impacts of reservoir operations (∼water supply) are particularly strong for the rivers crossing major irrigated areas of the world with the number of existing reservoirs including the Nile, the Orange, the Murray, the Mekong, the Ganges, the Indus, the Yangtze, the Huang He, the Mississippi, the Colorado, and the Columbia. Over these regions, reservoir operations generally increase the release during the low flow period to satisfy the water demands downstream. This alleviates the hydrological drought condition downstream. For river basins with the number of reservoirs with hydropower generation and flood control (e.g., Huang He, Dnieper, and Volga), the seasonal amplitude of simulated streamflow tends to decrease, which also reduces the frequency of hydrological occurrence. For other river basins such as the Orinoco, the Parana, the Danube, the Rhine, the Dnieper, the Elbe, the Congo, the Niger, and the Zambezi, simulated streamflow is less impacted by reservoir operations because of small reservoir capacity and lower water demands. For the Brahmaputra, reservoir capacity is low despite the large water demands (>50 km^3) and the low flow periods coincide with the growing season of irrigated crops (∼spring) which require large amounts of water. In this region, people are more vulnerable to hydrological droughts due to low buffering capacities. However, our scale of analysis (∼50 km by ∼50 km) does not comprehend local-scale adaptive response to drought; for example conjunctive use of surface water and groundwater, retention ponds, and water-saving practice (Grey and Sadoff 2007). Moreover, our modeling approach does not fully reflect regional agricultural practice in which farmers may adapt to drought conditions in order to reduce the water demands during the growing season, which may result in different cropping calendars and extents (e.g., different sowing times and crop growing seasons, length, and areas). These local-scale interventions and processes involved in drought resilience that operate well below the scale of our analysis are not accounted for, but play a vital role for enhancing the societal resistance to droughts.

Moreover, severe hydrological drought conditions aggravate groundwater overdraft, resulting in groundwater depletion over large irrigated regions (Scanlon *et al* 2012), e.g. western and central US, western Mexico, India, Pakistan, China, and Iran. This increased groundwater overdraft compensates, albeit temporarily, for decreased surface water availability (Taylor *et al* 2013).

In general, observed streamflow is used to derive an assessment of hydrological drought occurrence since it is vital to have a correct estimate of the flow duration curve, i.e. minimum and maximum flow. When peak flow is poorly reproduced, there is likely a considerable mismatch in simulating drought events. However, observed data are not available at large spatial extents but it is defined only at gauging stations (e.g., GRDC stations), though hydrological drought can be as extensive as regional to continental scales. To overcome this limitation, and to be able to separate out the effects of human water consumption the modeling approach was used. Since our modeling approaches employ a series of assumptions and various input data, there are number of limitations and uncertainties inherent to this study.

We note that streamflow estimates and the corresponding 80-percentile flow, Q_{80}, can vary substantially among different global hydrological models and with different climate forcing (Gosling *et al* 2010, 2011, Haddeland *et al* 2011). In tables S3 and S4 (available at stacks.iop.org/ERL/8/034036/mmedia), we evaluated simulated monthly streamflow against available GRDC stations (www.bafg.de/GRDC). We considered simulated streamflow both under pristine conditions and under transient human water consumption, and compared average, minimum (low), and maximum (peak) streamflow derived from observed and simulated monthly streamflow. The effect of transient water consumption is clearly observable for the rivers crossing major irrigated areas of the world with the number of existing reservoirs including the Nile, the Orange, the Murray, the Mekong, the Ganges, the Indus, the Yangtze, the Huang He, the Mississippi, the Columbia, and the Volga. For the other river basins, the impact of human water consumption is less obvious, but still noticeable such as the Orinoco, the Parana, the Brahmaputra, the Danube, the Rhine, the Dnieper, and the Elbe. For the Amazon, the Congo, the Niger, the Zambezi, the Mckenzie, and the Lena, the river discharge is hardly affected because of lower human water consumption. For those river basins where human water consumption is large, the overall model performance (R^2 and *NSC*) improves when considering human water consumption, except the Ganges where our general model performance is low. This improvement is particularly evident for simulated minimum streamflow and for river basins where the low flow periods coincide with the large seasonal water demands, e.g. the growing season of irrigated crops (e.g., Orange, Murray, Brahmaputra, Indus, and Huang He). When including all available GRDC stations with long streamflow records (table S4), the comparison of observed

and simulated streamflow also show improved performance (slope and R^2) when including human water consumption, but the maximum (peak) streamflow is hardly affected. Simulated streamflow, monthly actual evapotranspiration, and monthly total terrestrial water storage were also evaluated against GRDC observations, the ERA40 re-analysis data, and the GRACE satellite observations, respectively in earlier work (van Beek *et al* 2011, Wada *et al* 2012), and showed generally good agreement with them across the globe.

Furthermore, we validated simulated deficit volumes against those derived from observed streamflow for major river basins of the world. The comparison showed generally good agreement for most of the basins, yet large discrepancies occurred when simulated streamflow failed to reproduce well the peak flow and seasonal variability, regardless of high correlation obtained from comparison of monthly streamflow. For example, over the Congo, both the timing and deficit volume are not always well reproduced by our model, despite the good correlation between simulated and observed monthly streamflow ($R^2 = 0.95$). For the Zambezi, although our simulated monthly streamflow does not compare well with observed monthly streamflow ($R^2 = 0.75, \alpha = 0.47$, and $NSC = -1.2$), simulated drought characteristics and deficit volumes agree relatively well with those derived from observed streamflow. This is likely due to the fact that our simulated monthly streamflow reproduces well peak flows relative to low flows (see also supplementary material, available at stacks.iop.org/ERL/8/034036/mmedia).

Note that the model does not include any artificial water diversions such as aqueducts and inter-basin water transfer. Such diversions can supply additional water to satisfy part of human water consumption. In this study, human water consumption is subtracted from simulated streamflow that is routed through natural drainage network only. This means that in some regions where extensive diversion works are present (the US, India and China) the reduction of streamflow due to human water consumption is likely overestimated.

Moreover, the results largely rely on the accuracy of calculated human water consumption. The methods which we used to estimate sectoral consumptive water in this study were tested, and the corresponding results were validated against available statistics and estimates in an earlier study (Wada *et al* 2011a). They showed that estimated total water consumption compare well to available statistics for most of the countries over the period 1960–2000 with R^2 ranging from 0.91 to 0.97. However, the estimates are uncertain over some countries such as Vietnam, Uruguay, El Salvador, Jamaica, Madagascar, and Trinidad and Tobago, where we underestimate the water consumption by 10–50%, and also Colombia, Estonia and Moldova, where we overestimate the water consumption by 10–40%. Validation of simulated consumptive water use (per sector) remains difficult due to a lack of reliable information in many regions of the world. A recent study by Anderson *et al* (2012) combined remotely sensed precipitation and satellite observations of evapotranspiration and groundwater depletion to estimate surface water consumption by irrigated agriculture in California's Central Valley. This approach may be promising and opens up new ways to measure surface water consumption, particularly over data poor regions.

Our results showed that the standardization of deficit volumes relative to the threshold level, Q_{80}, works well for various regions under different climates, particularly to index the relative changes of the intensity of hydrological droughts over large spatial regions, and over a long-term period (e.g., decades). However, the standardization procedure creates missing values for intermittent streams where $Q_{80} = 0$. This problem is less obvious in our analysis since we used monthly rather than daily streamflow. To fully resolve the problem, lower threshold level or exceedance percentiles can be applied (Fleig *et al* 2006, van Huijgevoort *et al* 2012). Woo and Tarhule (1994), and Tate and Freeman (2000) tested threshold levels ranging from Q_5 to Q_{20} for intermittent streams over Africa. van Huijgevoort *et al* (2012) applied different threshold levels based on different flow percentiles. In this study, we used Q_{80} globally since human water consumption is intrinsically linked to perennial streams. However, it is worth noting that soil moisture (i.e., green water) is the major source of global food production (~80%) (Falkenmark *et al* 2009, Hoff *et al* 2010), while rainfed agriculture is rarely assessed in the context of human water needs. Global food demand has been increasing consistently as a result of a growing world population. This may even increase the reliance to rainfed agriculture in near future. The focus on blue water resources (i.e., surface freshwater) underexposes the effects of climate variability on global food production met by rainfed agriculture.

Human water consumption is expected to increase further due to growing population and their food demands (Gleick 2000, Alcamo *et al* 2003a, Wada *et al* 2013). In addition, some studies (Lehner *et al* 2006, Feyen and Dankers 2009) suggest that due to global warming hydrological drought will become more severe by the end of this century. The resulting further intensification of hydrological drought will have considerable impacts on society and ecosystem services (Döll *et al* 2009, Rodriguez-Iturbe *et al* 2011). At the same time, it is clear that managing water consumption is one of the more important mechanisms that facilitate adaptive responses to cope with drought conditions. For instance, over Asia good water and land management practices have a potential to increase irrigation efficiency, which will in turn decrease the substantial amount of water used for irrigation (Gleick *et al* 2010, Foley *et al* 2011). Investing and improving water technology (e.g., recycling) has also a good potential to reduce water consumption (Vörösmarty *et al* 2010) in many rapidly developing countries where water is scarce.

Acknowledgments

We cordially thank two anonymous referees and one anonymous board member for their constructive and thoughtful suggestions, which substantially helped to improve the quality of the letter. YW was financially supported by Research Focus Earth and Sustainability of Utrecht University (Project FM0906: *Global Assessment of Water Resources*). NW was financed by User Support Space Research Grant

of the Netherlands Organization for Scientific Research (Contract number: NWO GO-AO/30). This research benefited greatly from the availability of invaluable data sets as acknowledged in the references.

References

Adam J C and Lettenmaier D P 2003 Adjustment of global gridded precipitation for systematic bias *J. Geophys. Res.* **108** 4257

Alcamo J, Döll P, Henrichs T, Kaspar F, Lehner B, Rösch T and Siebert S 2003a Global estimation of water withdrawals and availability under current and business as usual conditions *Hydrol. Sci. J.* **48** 339–48

Alcamo J *et al* 2003b Development and testing of the WaterGAP 2 global model of water use and availability *Hydrol. Sci. J.* **48** 317–37

Allen R G, Pereira L S, Raes D and Smith M 1998 Crop evapotranspiration—guidelines for computing crop water requirements *FAO Irrigation and Drainage Paper* vol 56 (Rome: FAO)

Anderson R G, Lo M-H and Famiglietti J S 2012 Assessing surface water consumption using remotely-sensed groundwater, evapotranspiration, and precipitation *Geophys. Res. Lett.* **39** L16401

Andreadis K M, Clark E A, Wood A W, Hamlet A F and Lettenmaier D P 2005 Twentieth-century drought in the conterminous United States *J. Hydrometeorol.* **6** 985–1001

Bergström S 1995 The HBV model *Computer Models of Watershed Hydrology* ed V P Singh (Highlands Ranch, CO: Water Resource Publications)

Bredehoeft J D 2002 The water budget myth revisited: why hydrogeologists model? *Ground Water* **40** 340–5

Chow V T, Maidment D R and Mays L W 1988 *Applied Hydrology* (New York: McGraw-Hill)

Christensen J H, Christensen O B, Lopez P, van Meijgaard E and Botzet M 1996 *The HIRHAM4 Regional Atmospheric Climate Model* vol 96-4 (Copenhagen: Danish Meteorological Institute)

Coles S 2001 *An Introduction to Statistical Modeling of Extreme Values* (London: Springer)

Corzo Perez G A, van Huijgevoort M H J, Voß F and van Lanen H A J 2011 On the spatio-temporal analysis of hydrological droughts from global hydrological models *Hydrol. Earth Syst. Sci.* **15** 2963–78

Dai A 2011 Drought under global warming: a review *WIREs Clim. Change* **2** 45–65

Dai A 2013 Increasing drought under global warming: reconciling observed and model-simulated changes *Nature Clim. Change* **3** 52–8

Dee D P *et al* 2011 The ERA-Interim reanalysis: configuration and performance of the data assimilation system *Q. J. R. Meteorol. Soc.* **137** 553–97

Döll P, Fiedler K and Zhang J 2009 Global-scale analysis of river flow alterations due to water withdrawals and reservoirs *Hydrol. Earth Syst. Sci.* **13** 2413–32

Döll P and Lehner B 2002 Validating of a new global 30-min drainage direction map *J. Hydrol.* **258** 214–31

Falkenmark M, Kijne J W, Taron B, Murdoch G, Sivakumar M V K and Craswell E 1997 Meeting water requirements of an expanding world population *Phil. Trans. R. Soc.* B **352** 929–36 (and discussion)

Falkenmark M, Rockström J and Karlberg L 2009 Present and future water requirements for feeding humanity *Food Secur.* **1** 59–69

Feyen L and Dankers R 2009 Impact of global warming on streamflow drought in Europe *J. Geophys. Res.* **114** D17116

Fleig A K, Tallaksen L M, Hisdal H and Demuth S 2006 A global evaluation of streamflow drought characteristics *Hydrol. Earth Syst. Sci.* **10** 535–52

Fleig A K, Tallaksen L M, Hisdal H and Hannah D M 2011 Regional hydrological drought in north-western Europe: linking a new Regional Drought Area Index with weather types *Hydrol. Process.* **25** 1163–79

Foley J A *et al* 2011 Solutions for a cultivated planet *Nature* **478** 337–42

Fuchs T, Schneider U and Rudolf B 2008 Development of the GPCC data base and analysis products *GPCC Annual Report for Year 2007* (Offenbach am Main: GPCC)

Gleick P H 2000 The changing water paradigm: a look at twenty-first century water resources development *Water Int.* **25** 127–38

Gleick P H 2010 Roadmap for sustainable water resources in southwestern North America *Proc. Natl Acad. Sci. USA* **107** 21300–5

Gleick P H, Christian-Smith J and Cooley H 2010 Water-use efficiency and productivity: rethinking the basin approach *Water Int.* **36** 784–98

Gosling S N, Bretherton D, Haines K and Arnell N W 2010 Global hydrology modelling and uncertainty: running multiple ensembles with a campus grid *Phil. Trans. R. Soc.* A **368** 4005–21

Gosling S N, Taylor R G, Arnell N W and Todd M C 2011 A comparative analysis of projected impacts of climate change on river runoff from global and catchment-scale hydrological models *Hydrol. Earth Syst. Sci.* **15** 279–94

Grey D and Sadoff C W 2007 Sink or Swim? Water security for growth and development *Water Policy* **9** 545–71

Haddeland I *et al* 2011 Multimodel estimate of the global terrestrial water balance: setup and first results *J. Hydrometeorol.* **12** 869–84

Hagemann S and Gates L D 2003 Improving a sub-grid runoff parameterization scheme for climate models by the use of high resolution data derived from satellite observations *Clim. Dyn.* **21** 349–59

Hidalgo H G, Piechota T C and Dracup J A 2000 Alternative principal components regression procedures for dendrohydrologic reconstructions *Water Resour. Res.* **36** 3241–9

Hisdal H, Stahl K, Tallaksen L M and Demuth S 2001 Have streamflow drughts in Europe become more sever or frequent? *Int. J. Climatol.* **21** 317–33

Hisdal H and Tallaksen L M 2003 Estimation of regional, meteorological and hydrological drought characteristics: a case study for Denmark *J. Hydrol.* **281** 230–47

Hisdal H and Tveito O E 1993 Extension of runoff series using empirical orthogonal functions *Hydrol. Sci. J.* **38** 33–49

Hoff H, Falkenmark M, Gerten D, Gordon L, Karlberg L and Rockström J 2010 Greening the global water system *J. Hydrol.* **384** 177–86

Katz R W, Parlange M B and Naveau P 2002 Statistics of extremes in hydrology *Adv. Water Resour.* **25** 1287–304

Kraaijenhoff van de Leur D 1958 A study of non-steady groundwater flow with special reference to a reservoir coefficient *De Ingenieur* **70** 87–94

Krasovskaia I and Gottschalk L 1995 Analysis of regional drought characteristics with empirical orthogonal functions *New Uncertainty Concepts in Hydrology and Water Resources* (*International Hydrology Series*) ed Z W Kundezewicz (Cambridge: Cambridge University Press) pp 163–7

Lehner B and Döll P 2004 Development and validation of a global database of lakes, reservoirs and wetlands *J. Hydrol.* **296** 1–22

Lehner B, Döll P, Alcamo J, Henrichs T and Kasper F 2006 Estimating the impact of global change on flood and drought risks in Europe: a continental integrated analysis *Clim. Change* **75** 273–99

MacDonald G M 2010 Water, climate change, and sustainability in the southwest *Proc. Natl Acad. Sci. USA* **107** 21256–62

Mishra A K and Singh V P 2010 A review of drought concepts *J. Hydrol.* **391** 202–16

Mitchell T D and Jones P D 2005 An improved method of constructing a database of monthly climate observations and associated high-resolution grids *Int. J. Clim.* **25** 693–712
Mitosek H T 1995 Climate variability and change within the discharge time series: a statistical approach *Clim. Change* **29** 101–16
National Climatic Data Center 1990 *National Climate Information Disc 1* Data Reference (Washington, DC: National Climatic Data Center)
New M, Lister D, Hulme M and Makin I 2002 A high-resolution data set of surface climate over global land areas *Clim. Res.* **21** 1–25
Pederson N 2012 A long-term perspective on a modern drought in the American Southeast *Environ. Res. Lett.* **7** 014034
Peters E, Bier G, van Lanen H A J and Torfs P J J F 2006 Propagation and spatial distribution of drought in a groundwater catchment *J. Hydrol.* **321** 257–75
Rees G and Demuth S 2000 The application of modern information system technology in the European FRIEND project, Moderne Hydrologische Informationssysteme *Wasser und Boden* **52** 9–13
Roald L A, Wesselink A J, Arnell N W, Dixon J M, Rees H G and Andrews A J 1993 European water archive *Flow Regimes from International Experimental and Network Data (FRIEND)* ed A Gustard (Wallingford: Institute of Hydrology) pp 7–20
Rodriguez-Iturbe I, Caylor K and Rinaldo A 2011 Metabolic principles of river basin organization *Proc. Natl Acad. Sci. USA* **108** 11751–5
Seager R 2007 The turn of the century North American drought: global context, dynamics, and past analogs *J. Clim.* **20** 5527–52
Seibert J 1997 Estimation of parameter uncertainty in the HBV model *Nord. Hydrol.* **28** 247–62
Scanlon B R, Longuevergne L and Long D 2012 Ground referencing GRACE satellite estimates of groundwater storage changes in the California Central Valley, USA *Water Resour. Res.* **48** W04520
Shamsudduha M, Taylor R G, Ahmed K M and Zahid A 2011 The impact of intensive groundwater abstraction on recharge to a shallow regional aquifer system: evidence from Bangladesh *Hydrogeol. J.* **19** 901–16
Sheffield J and Wood E F 2007 Characteristics of global and regional drought, 1950–2000: analysis of soil moisture data from off-line simulation of the terrestrial hydrologic cycle *J. Geophys. Res.* **112** D17115
Sheffield J and Wood E F 2011 *Drought: Past Problems and Future Scenarios* (London: Earthscan) p 210
Sheffield J, Wood E F and Roderick M L 2012 Little change in global drought over the past 60 years *Nature* **491** 435–8
Soulé P T and Yin Z Y 1995 Short- to long-term trends in hydrologic drought conditions in the contiguous United States *Clim. Res.* **5** 149–57
Tallaksen L M, Hisdal H and van Lanen H A J 2009 Space–time modeling of catchment scale drought characteristics *J. Hydrol.* **375** 363–72
Tallaksen L M, Madsen H and Clausen B 1997 On the definition and modelling of streamflow drought duration and deficit volume *Hydrol. Sci. J.* **42** 15–33
Tallaksen L M and van Lanen H A J (ed) 2004 *Hydrological Drought: Processes and Estimation Methods for Streamflow and Groundwater* (*Developments in Water Science* vol 48) (Amsterdam: Elsevier Science BV)
Tate E L and Freeman S N 2000 Three modelling approaches for seasonal streamflow droughts in southern Africa: the use of censored data *Hydrol. Sci. J.* **45** 27–42
Taylor R G *et al* 2013 Groundwater and climate change *Nature Clim. Change* **3** 322–9
Timilsena J, Piechota T C, Hidalgo H and Tootle G 2007 Five hundred years of hydrological drought in the Upper Colorado River Basin *J. Am. Water Resour. Assoc.* **43** 798–812
Trenberth K E, Branstator G W and Arkin P A 1988 Origins of the 1988 North American drought *Science* **242** 1640–5
Uppala S M *et al* 2005 The ERA-40 re-analysis *Q. J. R. Meteorol. Soc.* **131** 2961–3012
van Beek L P H, Wada Y and Bierkens M F P 2011 Global monthly water stress: I. Water balance and water availability *Water Resour. Res.* **47** W07517
van der Knijff J, Younis J and de Roo A 2010 LISFLOOD: a GIS-based distributed model for river-basin scale water balance and flood simulation *Int. J. Geogr. Inf. Sci.* **24** 189–212
van Huijgevoort M H J, Hazenberg P, van Lanen H A J and Uijlenhoet R 2012 A generic method for hydrological drought identification across different climate regions *Hydrol. Earth Syst. Sci.* **16** 2437–51
van Loon A F and van Lanen H A J 2012 A process-based typology of hydrological drought *Hydrol. Earth Syst. Sci.* **16** 1915–46
Vörösmarty C J *et al* 2010 Global threats to human water security and river biodiversity *Nature* **467** 555–61
Wada Y, van Beek L P H and Bierkens M F P 2011a Modelling global water stress of the recent past: on the relative importance of trends in water demand and climate variability *Hydrol. Earth Syst. Sci.* **15** 3785–808
Wada Y, van Beek L P H and Bierkens M F P 2012 Nonsustainable groundwater sustaining irrigation: a global assessment *Water Resour. Res.* **48** W00L06
Wada Y, van Beek L P H, van Kempen C M, Reckman J W T M, Vasak S and Bierkens M F P 2010 Global depletion of groundwater resources *Geophys. Res. Lett.* **37** L20402
Wada Y, van Beek L P H, Viviroli D, Dürr H H, Weingartner R and Bierkens M F P 2011b Global monthly water stress: 2. Water demand and severity of water stress *Water Resour. Res.* **47** W07518
Wada Y *et al* 2013 Multimodel projections and uncertainties of irrigation water demand under climate change *Geophys. Res. Lett.* at press (doi:10.1002/grl.50686)
Weedon G P *et al* 2011 Creation of the WATCH forcing data and its use to assess global and regional reference crop evaporation over land during the twentieth century *J. Hydrometeorol.* **12** 823–48
Wilhite D A (ed) 2000 *Drought: A Global Assessment* (London: Routledge)
Wilhite D A and Glantz M H 1985 Understanding the drought phenomenon: the role of definitions *Water Int.* **10** 111–20
Wisser D, Fekete B M, Vörösmarty C J and Schumann A H 2010 Reconstructing 20th century global hydrography: a contribution to the Global Terrestrial Network-Hydrology (GTN-H) *Hydrol. Earth Syst. Sci.* **14** 1–24
Woo M and Tarhule A 1994 Streamflow droughts of northern Nigerian rivers *Hydrol. Sci. J.* **39** 19–34
Zelenhasić E and Salvai A 1987 A method of streamflow drought analysis *Water Resour. Res.* **23** 156–68